

Experimental investigation of particle dissolution rates in aqueous solutions for hydrogen production

O. A. Jianu¹ · Z. Wang¹ · M. A. Rosen¹ · G. F. Naterer²

Received: 3 November 2014 / Accepted: 23 November 2015 / Published online: 28 November 2015
© Springer-Verlag Berlin Heidelberg 2015

Abstract Results of reaction kinetics studies of chemical processes related to materials integration of the thermochemical copper-chlorine cycle for hydrogen production are reported. The reaction rate of solid cuprous chloride (CuCl) in liquid hydrochloric acid is investigated experimentally for various acid concentrations. A rate constant—a function of constituent concentrations—describes how quickly the reactants are converted into products in satisfying the activation energy to enable the reaction to move forward. In this paper, the change in area of a solid CuCl particle is examined, rather than concentration in previous studies. New predictive models are developed to describe the characteristics of the chemical reaction in terms of its transition states and reaction mechanisms.

1 Introduction

Thermochemical cycles are promising alternatives for large-scale hydrogen production. In recent years, the

copper-chlorine (Cu-Cl) cycle has increasingly attracted the interest of engineers and scientists due to its lower temperature input (i.e. below 550 °C) than most other thermochemical cycles (i.e. above 650 °C) [1–5]. A schematic of a thermochemical Cu-Cl cycle for water splitting showing overall inputs, outputs and required temperatures for operation is illustrated in Fig. 1.

Thermochemical water decomposition generally involves at least three distinct steps: hydrogen production, oxygen production and recycling [1]. The advantage of this cycle is that chemical reactions form a closed internal loop and recycle all chemicals on a continuous basis, without emitting any greenhouse gases externally to the atmosphere [6–9].

In the first step of the cycle, hydrogen is generated from an electrochemical reaction given by:



The efficiency of the electrolytic cell depends on the electrode materials and their ability to produce hydrogen at low potentials, on the performance of the membrane and on the concentration and temperature of electrolytic solution [6].

The second step of the cycle involves removal of the water from aqueous cupric chloride. Different methods have been investigated with crystallization being considered as an effective method to recover solids from solution, due to its relatively low energy utilization, low material requirements and lower cost compared to other alternatives.

The third step involves supplying the water-free CuCl₂ solid to the hydrolysis reactor to produce copper oxychloride (Cu₂OCl₂) and HCl gas [7]. This is achieved in an endothermic non-catalytic gas–liquid or gas–solid reaction, expressible by the following equation:



✉ O. A. Jianu
Ofelia.Jianu@uoit.ca

Z. Wang
Forest.Wang@uoit.ca

M. A. Rosen
Marc.Rosen@uoit.ca

G. F. Naterer
gnaterer@mun.ca

¹ Faculty of Engineering and Applied Science, University of Ontario Institute of Technology, 2000 Simcoe Street North, Oshawa, ON L1H 7K4, Canada

² Faculty of Engineering and Applied Science, Memorial University of Newfoundland, 240 Prince Phillip Drive, St. John's, NF A1B 3X5, Canada

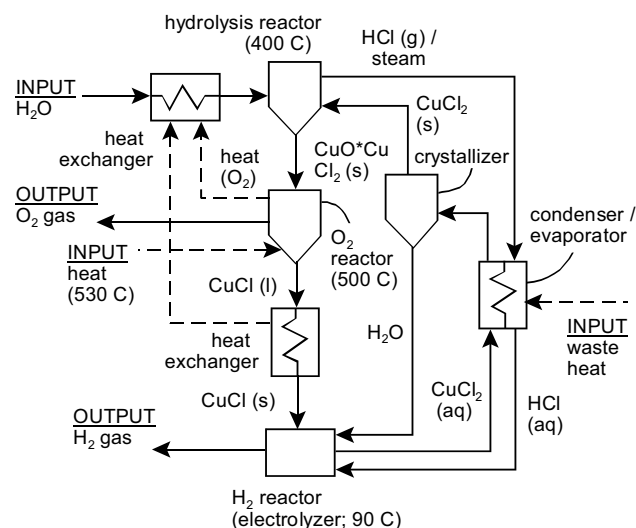
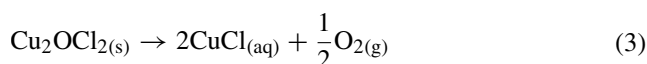


Fig. 1 Schematic of a thermochemical Cu-Cl cycle showing input and output requirements

The chemical equilibrium and gaseous product fraction of this reaction predict the ability to effectively integrate the hydrolysis reactor and the downstream electrolytic process as indicated by Eq. (1).

The last step in the cycle is the decomposition reaction. This reaction is expressed by:



This is a decomposition reaction in which gaseous oxygen and molten CuCl are obtained from copper oxychloride. Several gaseous products exit the reactor such as oxygen, CuCl vapour and some products from side reactions such as HCl gas, Cl₂ gas and water vapour. When particles enter the reactor at a temperature below 430 °C, bubbles may develop in the molten salt. These bubbles and their aggregate formation decrease the contact area between the reactant particle and heating medium; therefore, aggregations may float to the surface. This may be a major safety concern, as reported in Ref. [1]. A model to predict the amount of mass transferred into the bubbles has been reported in [9].

For successful operation of the Cu-Cl cycle for hydrogen production, it is important to effectively design intermediate processes that aid in the integration of the main steps. Molten CuCl salt leaves the oxygen reactor, enters an intermediate step that recovers heat thus changing its state to solid, and finally reaches the electrolysis reactor where it aids in the production of hydrogen. Similarly, HCl gas leaves the hydrolysis reactor and enters the electrolysis reactor as hydrochloric acid. For improved performance of the cycle, it is necessary to dissolve the solid CuCl particles in aqueous HCl before reaching the electrolysis cell.

Hence, a second intermediate step is required between the oxygen reactor and electrolysis reactor. Before introducing this step, a series of experiments have been performed to understand the dynamics of solid CuCl particles in aqueous HCl. Since HCl volatility increases with concentration and temperature, this step will be performed at temperatures close to room temperature to minimize the escape of HCl. A better understanding of the dynamics of the particles and the dissolution rates will aid in the design of the mixing step and effective integration of the cycle. Experiments have been performed and results are presented in Sect. 3.

In liquid–solid flows, there is a liquid continuum carrying dispersed solids which are suspended in the liquid phase due to drag and pressure forces. These types of flows form slurry flows and comprise two different aspects: one that regards the mixture as a whole and another that is the relative flow between solid particles and the liquid. One key aspect of solid–liquid flows is to understand the particle’s behavior in the mixture; that is, whether particles distribute evenly within the mixture and remain suspended or segregate and deposit. Researchers have found that there is a tendency towards segregation in vertical flows which is due to symmetrical configurations of forces. A uniform solid distribution can be expected as long as the condition for conveyance is satisfied. It was also found that the only particles that can be kept suspended without any turbulence have $\text{Re} < 10^{-6}$ and they are conveyed by Brownian molecular movement [10]. To have particle suspension, the ratio of the settling velocity of the particles and fluid velocity must be kept constant. In this paper, the critical settling velocity of coarse particles is investigated in order to determine a fluid velocity that would keep the particles suspended. This is a necessary condition to ensure CuCl particles dissolve evenly in aqueous HCl and the dissolution rate is accelerated.

In dissolution, a solute dissolves in a solvent to form a solution. In this process, the solute’s structure is disintegrated into separate ions, atoms and molecules. This is governed by thermodynamics and kinetics. The outcome of the process is limited by the heat of solution and entropy of solution while the dissolution itself is a kinetic process and not governed by such energies. Solubility is defined by the saturated concentration of solute in a solution, which is determined by the thermodynamic limit. Dissolution is not always an instantaneous process as it depends on the rate of diffusion and the surface area of the material.

Solubilities of solids in liquids are required to determine mass transfer in liquid–solid systems. Studies of solubility of solid cuprous chloride (CuCl) in aqueous hydrochloric acid (HCl and H₂O) have been reported in past literature [11–13]. Shashikant et al. [11] investigated the solubility in an oxygen free environment since the presence of oxygen may oxidate the cuprous salt CuCl to soluble cupric

salts containing Cu^{2+} . O'Connor et al. [12] performed solubility experiments in order to determine a solubility curve. Their study investigated the conversion rate from CuCl to CuCl_2 ions in order to determine the crystal size of chloro complexes. Frits investigated the solubility in order to determine the equilibrium constants for formation and a set of virial parameters representing the activity coefficients of the ions formed in dissolution [13]. The oxidation of CuCl by O_2 in aqueous HCl has been studied in order to clarify the kinetics of chemical absorption of O_2 in the aqueous ternary system. Gavriš and Galinker [14] compared the dissolution of CuCl in water and aqueous HCl , then determined that even a relatively low concentration of HCl (0.6 M) can significantly increase the solubility of CuCl .

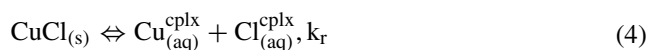
Researchers have been developing techniques to monitor reactions over small timescales in the range of femtoseconds to large timescales over hours or days. It is relatively straightforward to monitor the kinetics of a slow reaction and challenging to monitor fast reactions, which in general require highly specialized techniques for accurate monitoring. In general, kinetics experiments consist of initiating a reaction by mixing the reactants, however, the timescale of the initiation is negligible relative to that of the reaction. Once the reaction is initiated, the concentrations of the reactants and products are monitored. Most of the techniques studied by researchers are batch or continuous. In batch techniques, concentrations are monitored as a function of time after the reaction is initiated. In a continuous technique, the reaction initiation occurs on a continuous basis and the different concentration regions in the reaction vessel infer to the reaction mixture composition and time [15–17].

Mass transfer occurs between liquid and solid during dissolution. The driving force of dissolution of a particle is limited by thermodynamic equilibrium, which relates to the solubility. The reactant system between the decomposition reactor and electrolysis of the Cu-Cl cycle is a ternary system involving CuCl , HCl and H_2O . For integration of the decomposition reactor with the electrolytic cell, it is necessary to determine the solubility equilibrium. Hence, the objective of this investigation is to examine the dissolution rate of solid CuCl in aqueous HCl solution experimentally. Since the dissolution of solid CuCl in aqueous HCl is not easy to be observed by human eyes, a different method of monitoring the rate was utilized. In this paper, the reaction was initiated and the size of particles was monitored via a camera system. The dissolution of CuCl in aqueous HCl is an important auxiliary process of the thermochemical Cu-Cl cycle for hydrogen production, as the reactor integration design depends on determining the reaction kinetics. The findings could be used for matching the material flows in the integration of the decomposition reactor with

the anode of the electrolysis cell in the thermochemical Cu-Cl cycle for hydrogen production.

2 Dissolution and reaction model

The dissolution of solid CuCl particle in aqueous HCl could be described as a special case of a chemical reaction wherein the chemical species react directly to form products. This process is given by:



where k_r is the rate constant.

The rate constant k_r describes how fast a chemical process reaches equilibrium; that is how fast the reactants are converted into products by overcoming the activation energy enabling the reaction to move forward. Without overcoming the activation energy, the reaction would not take place as shown in the previous section (i.e. CuCl does not dissolve in a binary system at low temperature and the dissolution rate increases with the increase in concentration of HCl). The reaction rate k_r and the kinetic energy required for activation of the reaction describes how fast this reaction will reach equilibrium (i.e. the maximum reaction extent).

Therefore, the integrated rate law of a first-order reaction is:

$$\ln[\text{CuCl}]_t = -k_r t + \ln[\text{CuCl}]_0 \quad (5)$$

Equation (5) can be rearranged as follows:

$$\ln\left(\frac{[\text{CuCl}]_t}{[\text{CuCl}]_0}\right) = -k_r t \quad (6)$$

Solving Eq. (6) results in:

$$[\text{CuCl}]_t = [\text{CuCl}]_0 e^{-k_r t} \quad (7)$$

Where $[\text{CuCl}]_0$ is the initial concentration of CuCl , $[\text{CuCl}]_t$ is the concentration of CuCl at time t , k_r is the rate constant and t is elapsed time. This analysis is applied in Sect. 4. However, the change in area of the solid CuCl particle is examined, rather than the concentration. Also, it is important to note that the proposed model in Eq. (5) only accounts for the forward reaction of the system.

3 Experimental setup

An experimental apparatus has been designed and built at the University of Ontario Institute of Technology (UOIT) in the Clean Energy Research Laboratory (CERL) to investigate dissolution rates of solid CuCl in aqueous HCl . The experimental apparatus consists of an 8-in high, 4-in

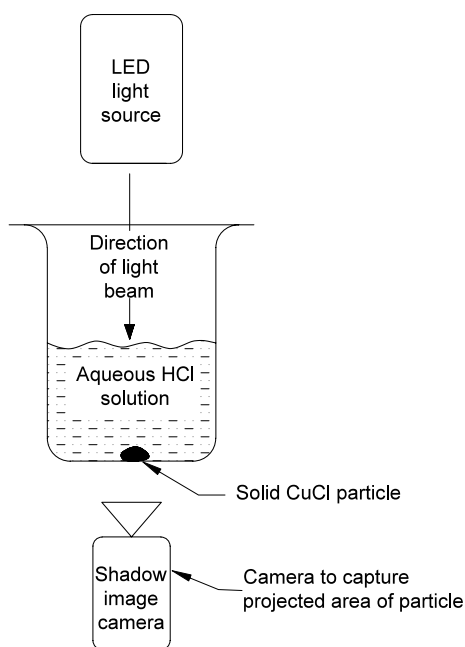


Fig. 2 Experimental setup for dissolution rate

diameter clear Pyrex vessel filled with liquid and a camera system (see Fig. 2). The experimental setup design and construction are described in detail in Ref. [18]. The setup was designed based on Refs. [19–21] so that the uncertainty associated with the experiment can be minimized. The experimental error introduced due to the equipment and analysis as well as the deviation is shown in Table 1. It is observed that the highest error is due to calibration of the camera. In order to minimize this error, a calibration technique suggested in [22–24] was employed and compared with the calibration technique presented in DynamicStudio software.

Irregular shaped particles with a mass of ~7 mg are dropped in HCl solution. Due to a difference in concentration, molecular diffusion takes place until equilibrium is achieved. However, it has been observed that the molecular diffusion is significantly slowed down due to local saturation. Methods for enhancing the dissolution rate are sought since a faster dissolution rate is desirable for the process integration of the Cu-Cl cycle. Therefore, the research group has investigated the introduction of nitrogen to aid in the mixing of the solution for an improved dissolution rate. The effect of mixing through gas cross-flow and counter-flow for different injection angles has been reported [25–27]. Hence, in this set of experiments, nitrogen gas is supplied from the bottom of the Pyrex vessel. Nitrogen was supplied at a flow rate of 4L/min. This flow generated some turbulence in the liquid to reduce the local saturation of dissolved CuCl, however it was assumed small relative to the magnitude to significantly disturb the motion of particles.

Table 1 Mean relative error of the reaction kinetics predictive model

Phase	Molarity (M)	Number of data points	Mean relative error (%)
Liquid–Solid	6	4	2.71
	9	5	12.68
	12	5	28.39
Gas–Liquid–Solid	6	4	4.87
	9	5	4.64
	12	5	6.49

4 Results and discussion

As described in the previous section, solid CuCl particles of the same mass (i.e. 7 mg) were dropped into quiescent HCl solution and the change in area was recorded. Figures 3, 4 and 5 illustrate the change in area for particles dissolving in 6 M, 9 M and 12 M HCl solution, respectively, where M is the molarity of the solution. It is important to note that although the particles have the same mass, the projected area recorded by the camera is different due to the irregular shape of the particles. Figure 3 shows the particle dissolution in 6 M HCl whereas the model is reported in Ref. [18]. A model for particle dissolution in 9 M HCl quiescent solution (Fig. 4) is obtained which has the following form:

$$A_{9M} = 12.97 \times e^{-0.00057t} \quad (8)$$

where A_{9M} represents the surface area of particle dissolving in 9 M HCl, and t is the time. This representation returned an R-squared value of 0.9801, which indicates a good correlation between the variables. Also, it can be estimated that a decrease in area from 12.60 mm² to 4.86 mm² would take about 1500 s. Similarly, a model for particle dissolution in 9 M HCl solution with mixing is obtained which is of the following form:

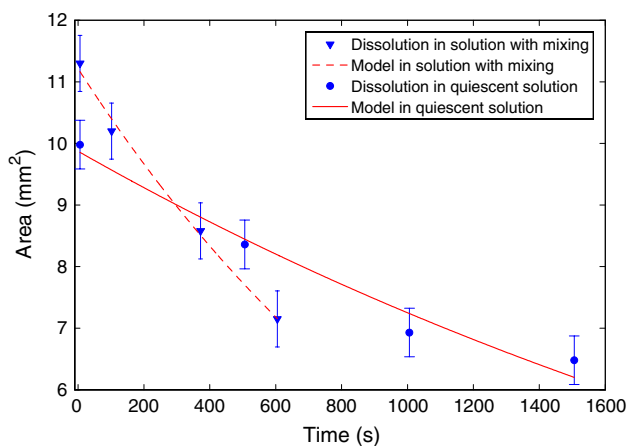


Fig. 3 Comparison of CuCl particle dissolution in a 6 M HCl quiescent solution and solution with mixing

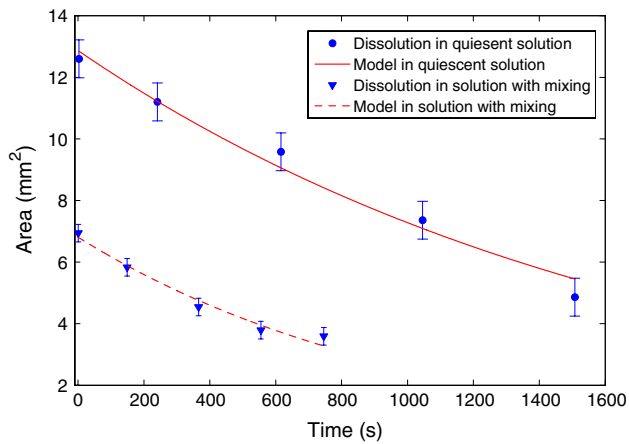


Fig. 4 Comparison of CuCl particle dissolution in a 9 M HCl quiescent solution and solution with mixing

$$A_{9M_{\text{mix}}} = 6.809 \times e^{-0.00098t} \quad (9)$$

where $A_{9M_{\text{mix}}}$ represents the surface area of particle dissolving in 9 M HCl solution with mixing. This representation returned an R-squared value of 0.9762, which indicates a good correlation between the points. Also, it can be estimated that a decrease in area from 6.94 mm² to 3.59 mm² takes about 750 s.

The change in area for 12 M HCl solution is obtained by the same procedure. From Fig. 5 it can be noted that the solid particle's area change follows an exponential decrease given by:

$$A_{12M} = 9.706 \times e^{-0.00083t} \quad (10)$$

where A_{12M} represents the surface area, and t is the time. This representation returned an R-squared value of 0.9811, which indicates a good correlation between the variables. Also, a change in area from 9.62 mm² to 3.43 mm² took about 1100 s.

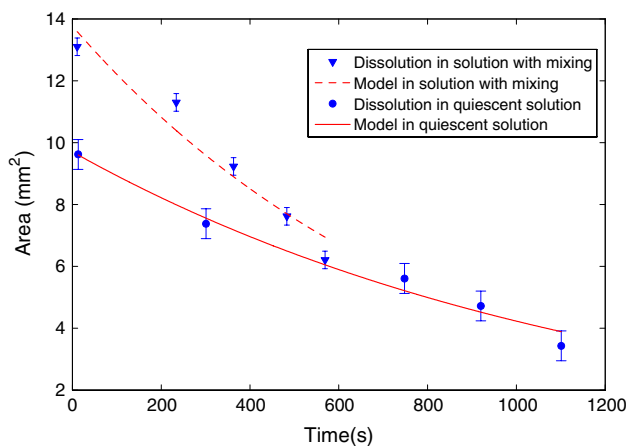


Fig. 5 Comparison of CuCl particle dissolution in a 12 M HCl quiescent solution and solution with mixing

Finally, dissolution of solid CuCl particle in 12 M HCl solution with mixing and the change in projected area is given by:

$$A_{12M_{\text{mix}}} = 13.77 \times e^{-0.0012t} \quad (11)$$

This returned R-squared value of 0.9438 indicates a good correlation between the points. From Fig. 5, it is estimated that a change in projected area of the particle from 13.1 mm² to 6.21 mm² takes about 560 s. Therefore, when nitrogen bubbles are introduced as a mixing agent, the time to dissolve particles decreases by about 50 %.

A relationship between the exponents as a function of concentration of HCl is needed. Through a semi-mechanistic approach based on non-linear least square method, a relationship for the exponents was determined as follows:

$$k_{r,q} = -8.696 \cdot 10^{-5} \times [\text{HCl}] + 0.00021 \quad (12)$$

where $k_{r,q}$ describes the dissolution rate in quiescent HCl solution.

Also, it is noted that constants 12.970 and 9.706 in Eq. (8) and (10) are the initial projected areas of the CuCl particles in 9 M and 12 M quiescent HCl solution, respectively, whereas the initial area for the 6 M HCl solution is obtained from Ref. [18]. Therefore, an expression for the change in area of CuCl particles in quiescent HCl solution is given by:

$$A_{t,q} = A_0 e^{-k_{r,q}t} \quad (13)$$

where $A_{t,q}$ is the projected area changing as a function of time t in quiescent solution, A_0 is the initial area and $k_{r,q}$ is given by Eq. (12).

Similar to the procedure described for particles dissolving in quiescent solution, it is necessary to obtain a relationship describing the exponents in terms of HCl concentration. The same semi-mechanistic model described above was applied to determine a relationship as follows:

$$k_{r,m} = 7.671 \cdot 10^{-5} \times [\text{HCl}] + 0.00029 \quad (14)$$

Also, constants 6.809 and 13.770 in Eq. (9) and (11) are the initial projected areas of the particles dissolving in 9 M and 12 M solution with mixing, respectively, whereas the initial area for 6 M solution is obtained from Ref. [18]. Therefore, a relationship describing the change of area for different HCl molarities in the presence of mixing is obtained as follows:

$$A_{t,m} = A_0 e^{-k_{r,m}t} \quad (15)$$

where $A_{t,m}$ is the area changing with time t in the presence of mixing, A_0 is the initial projected area of the particle and $k_{r,m}$ is given by Eq. (14).

In order to evaluate the performance of the model, the mean relative error η was calculated. The performance of

Table 2 Particle dynamics results

R_{maj} (mm)	R_{min} (mm)	Sphericity (ψ)	Re_s	C_D	Settling velocity, v_t (m/s)	Hindered settling velocity, v_s (m/s)
1.220	0.550	0.886	982.25	0.55	0.48	0.31
1.499	0.694	0.893	70.52	1.22	0.37	0.21
0.831	0.531	0.963	704.39	0.58	0.43	0.36
1.096	0.965	0.997	80.76	1.14	0.38	0.37
1.672	0.633	0.836	76.41	1.17	0.38	0.23
1.266	0.299	0.681	37.64	1.69	0.24	0.13
0.878	0.534	0.954	29.36	1.96	0.24	0.21
1.209	0.440	0.824	41.54	1.60	0.27	0.17
1.235	0.397	0.784	51.85	1.42	0.28	0.16
1.219	0.892	0.982	81.40	1.14	0.38	0.35
1.476	0.539	0.825	54.81	1.38	0.32	0.19
1.398	0.689	0.909	60.61	1.31	0.35	0.27
0.921	0.737	0.991	71.79	1.21	0.33	0.30
1.113	0.643	0.945	56.05	1.36	0.32	0.27
1.326	0.960	0.981	113.72	0.99	0.43	0.39
0.988	0.709	0.980	80.22	1.15	0.34	0.32
1.217	0.892	0.982	90.65	1.08	0.39	0.36
1.411	1.360	1.000	108.90	1.00	0.47	0.47
1.749	0.846	0.905	87.90	1.10	0.42	0.31
1.564	0.915	0.947	88.02	1.10	0.42	0.35
1.999	1.514	0.986	181.88	0.83	0.58	0.54
1.334	0.949	0.979	126.72	0.94	0.44	0.40
2.080	0.923	0.882	114.72	0.98	0.48	0.44
1.884	1.415	0.985	157.88	0.87	0.55	0.51

the model at different HCl concentrations, with and without mixing is summarized in Table 1.

The main forces acting on the falling particles are gravitational, buoyancy and drag. When particles are in motion, the drag force, which is a function of particle's velocity, opposes the gravitational force. The particle's velocity increases until the gravitational force is balanced by the drag force and buoyancy at which point there is no further change in a particle's velocity and this velocity is referred to as the terminal velocity. A falling particle's terminal velocity is affected by parameters altering the drag; therefore the terminal velocity is most notably dependent upon a particle's size, shape (e.g. sphericity) and density. Also, drag is affected by fluid properties such as viscosity and density.

The behavior of spherical particles in a fluid can be described by Stokes, transitional and Newtonian settling models. However, these models have limitations in practical applications since the walls of the vessel and other particles can also affect particle's velocity. Therefore, it is important to consider the interaction of particles in the fluid, or the interaction of the particles with the container

walls in practical applications such as the copper-chlorine cycle. For this reason, a hindered settling velocity was considered in the analysis of particle dynamics for improved dissolution. The hindered settling velocity was calculated using the model of Webber [10]. In the first step, Re_s was calculated based on particle's instantaneous velocity recorded by the camera. The setup to record the particle velocity is described in detail in Ref. [18]. Once Re_s was determined, the particle terminal velocity and sphericity were calculated. Lastly, the hindered settling velocity of the particle was obtained and tabulated in Table 2. It can be observed that the hindered settling velocity ranges from about 0.27 to 0.63 m/s for the tested particles. Therefore, for all the particles to be suspended, the flow velocity must be much greater than the upper range of the hindered settling velocity.

5 Conclusions

New experimental data on the particle dissolution kinetics associated with cuprous chloride dissolution in

hydrochloric acid have been reported in this paper. Correlations were developed to provide new insight about the concentration of the solution and the dependence of the change in area of the particle on time and concentration. Results were presented for different concentrations in quiescent and mixed solutions. These results aid in the integration of material streams of the thermochemical Cu-Cl cycle for hydrogen production.

Acknowledgments Financial support from the Ontario Research Excellence Fund and Canadian Nuclear Laboratories (formerly Atomic Energy of Canada Limited; AECL) is gratefully acknowledged.

References

- Naterer G, Suppiah S, Lewis M, Gabriel K, Dincer I, Rosen MA et al (2009) Recent Canadian advances in nuclear-based hydrogen production and the thermochemical Cu-Cl cycle. *Int J Hydrogen Energy* 34:2901–2917
- Naterer GF, Suppiah S, Stolberg L, Lewis M, Ahmed S, Wang Z, Rosen MA, Dincer I, Gabriel K, Secnik E, Easton EB, Lvov SN, Papangelakis V, Odukoya A (2009) Progress of international program on hydrogen production with the copper-chlorine cycle. *Int J Hydrogen Energy* 39:2431–2445
- Naterer GF, Suppiah S, Stolberg L, Lewis M, Ferrandon M, Wang Z et al (2011) Clean hydrogen production with the Cu-Cl cycle—Progress of international consortium, I: experimental unit operations. *Int J Hydrogen Energy* 35:15472–15485
- Suppiah S, Stolberg L, Boniface H, Tan G, McMahan S, York S, Zhang W (2010) Development of the medium-temperature Cu-Cl cycle and contributions to the high-temperature sulphur-iodine cycle. *Nucl Prod Hydrog* 4:66–75
- Rosen MA (2010) Advances in hydrogen production by thermochemical water decomposition: a review. *Energy* 35:1068–1076
- Kim S, Schatz R, Khurana S, Fedkin M, Wang C, Lvov S (2011) Advanced CuCl electrolyzer for hydrogen production via Cu-Cl thermochemical cycle. *ECS Trans* 35:257–265
- Naterer GF, Suppiah S, Stolberg L, Lewis M, Wang Z, Rosen MA, Dincer I, Gabriel K, Odukoya A, Secnik E, Easton EB, Papangelakis V (2015) Progress in thermochemical hydrogen production with the copper-chlorine cycle. *Int J Hydrogen Energy* 40:6283–6295
- Pope K, Wang ZL, Naterer GF, Secnik E (2012) Interfacial thermodynamics and X-ray diffraction of hydrolysis products in multiphase reacting flow of the Cu-Cl cycle. *Int J Hydrogen Energy* 37:15011–15019
- Jianu OA, Rosen MA, Naterer GF, Wang Z (2015) Two-phase bubble flow and convective mass transfer in water splitting processes. *Int J Hydrogen Energy* 40:4047–4055
- Weber M, Changeux J-P (1974) Binding of *Naja nigricollis* tritiated a-toxin to membrane fragments from *Electrophorus* and *Torpedo* electric organs: I: binding of the tritiated a-neurotoxin in the absence of effector. *Molec Pharmac* 10:1–14
- Kale SS, Tamhankar SS, Chaudhari RV (1979) Solubility of cuprous chloride in aqueous hydrochloric acid solutions. *J Chem Eng Data* 24:110–111
- O'Connor JJ, Thomasian A, Armington AF (1968) The analysis and solubility of cuprous chloride in hydrochloric acid solutions. *J Electrochem Soc: Electrochem Sci* 115(9):931–932
- Fritz J (1982) Solubility of cuprous chloride in various soluble aqueous chlorides. *J Chem Eng Data* 27:188–193
- Gavriš ML, Galinker IS, *Doklady Akademii Nauk SSSR* (1955) 102:89–91. (Cross-referred from: Valyashko V (2008) Hydrothermal properties of materials: experimental data on aqueous phase equilibria and solution properties at elevated temperatures and pressures. Wiley pp 33–34)
- Atkins WP (2011) *Physical chemistry*, 9th edn. Oxford University Press, USA
- Pilling MJ, Seakins PW (1996) *Reaction kinetics*, 2nd edn. Oxford University Press, USA
- Laidler KJ (1987) *Chemical kinetics*, 2nd edn. Harper & Row, New York
- Jianu OA, Wang Z, Rosen MA, Naterer GF (2013) Shadow imaging of particle dynamics and dissolution rates in aqueous solutions for hydrogen production. *Exp Thermal Fluid Sci* 51:297–301
- Moffat RJ (1982) Contributions to the theory of single-sample uncertainty analysis. *Trans ASME* 104:250–258
- Moffat RJ (1985) Using uncertainty analysis in the planning of an experiment. *J Fluids Eng* 107:173–178
- Kline SJ, McClintock FA (1953) Describing uncertainties in single-sample experiments. *Mech Eng* 75:3–8
- Nordin N, Othman S, Raghavan VR, Karim ZAA (2012) Verification of 3-D stereoscopic PIV operation and procedure. *Int J Eng Technol* 12:19–26
- Imre E, Guillemaut J-Y, Hilton A (2011) Calibration of nodal and free-moving cameras in dynamic scenes for post-production, center for vision, speech and signal processing. University of Surrey, Guildford, pp 260–267
- Zhang ZA (2000) Flexible new technique for camera calibration. *Pattern Anal Mach Intell* 22:1330–1334
- Bai B-F, Zhang H-B, Liu L, Sun H-J (2009) Experimental study on turbulent mixing of spray droplets in crossflow. *Exp Thermal Fluid Sci* 33:1012–1020
- Wang Q, Ma X, Lan Z, Chen J, Bai T (2012) Experimental study on mixing effect of falling film on coated division tube by thermal tracing technique. *Exp Therm Fluid Sci* 38:165–170
- Okorafor AA, He S, Morrison D (2012) Experimental investigation of three-dimensional flow in a double-diffusive interface system with lateral heating. *Exp Thermal Fluid Sci* 42:143–153